


## Article

# Highly Efficient Production of Furfural from Corncob by Barley Hull Biochar-Based Solid Acid in Cyclopentyl Methyl Ether–Water System

Bo Fan <sup>1</sup>, Linghui Kong <sup>1</sup> and Yucai He <sup>1,2,\*</sup> 

<sup>1</sup> School of Pharmacy & Biological and Food Engineering, Changzhou University, Changzhou 213164, China; fanboxiaoyu@cczu.edu.cn (B.F.); m18852654667@163.com (L.K.)

<sup>2</sup> State Key Laboratory of Biocatalysis and Enzyme Engineering, School of Life Sciences, Hubei University, Wuhan 430062, China

\* Correspondence: yucaihe@cczu.edu.cn

**Abstract:** Furfural, an important biobased compound, can be synthesized through the chemocatalytic conversion of *D*-xylose and hemicelluloses from lignocellulose. It has widespread applications in the production of valuable furans, additives, resins, rubbers, synthetic fibers, polymers, plastics, biofuels, and pharmaceuticals. By using barley hulls (BHs) as biobased support, a heterogeneous biochar Sn-NUS-BH catalyst was created to transform corncob into furfural in cyclopentyl methyl ether–H<sub>2</sub>O. Sn-NUS-BH had a fibrous structure with voids, a large comparative area, and a large pore volume, which resulted in more catalytic active sites. Through the characterization of the physical and chemical properties of Sn-NUS-BH, it was observed that the Sn-NUS-BH had tin dioxide (Lewis acid sites) and a sulfonic acid group (Brønsted acid sites). This chemocatalyst had good thermostability. At 170 °C for 20 min, Sn-NUS-BH (3.6 wt%) was applied to transform 75 g/L of corncob with ZnCl<sub>2</sub> (50 mM) to generate furfural (80.5% yield) in cyclopentyl methyl ether–H<sub>2</sub>O (2:1, *v/v*). This sustainable catalytic process shows great promise in the transformation of lignocellulose to furfural using biochar-based chemical catalysts.

**Keywords:** biochar heterogeneous catalyst; furfural; cyclopentyl methyl ether; ZnCl<sub>2</sub>; biomass



**Citation:** Fan, B.; Kong, L.; He, Y. Highly Efficient Production of Furfural from Corncob by Barley Hull Biochar-Based Solid Acid in Cyclopentyl Methyl Ether–Water System. *Catalysts* **2024**, *14*, 583. <https://doi.org/10.3390/catal14090583>

Academic Editor: Gartzzen Lopez

Received: 2 August 2024

Revised: 21 August 2024

Accepted: 29 August 2024

Published: 1 September 2024



**Copyright:** © 2024 by the authors. Licensee MDPI, Basel, Switzerland. This article is an open access article distributed under the terms and conditions of the Creative Commons Attribution (CC BY) license (<https://creativecommons.org/licenses/by/4.0/>).

## 1. Introduction

The swift depletion of global fossil fuel reserves, coupled with escalating environmental pollution and an intensifying energy crisis, has heightened the focus on developing and utilizing renewable energy sources [1]. Lignocellulosic biomass is a promising feedstock for manufacturing biofuels and other value-added chemicals due to its abundance, low cost, and potential to reduce greenhouse gas emissions compared to fossil fuels [2–6]. It primarily consists of lignin, hemicellulose, and cellulose [7]. Hemicellulose is one kind of non-cellulosic polysaccharide in the cell walls of plants [8], which can frequently be transformed into biobased chemicals such as furfural [9,10]. Furfural is a pivotal furan-based compound with extensive applications across various industries. It is widely utilized in the manufacturing of furans, disinfectants, plastics, flavors, resins, dyes, fine chemicals, and biofuels, and it also serves as an industrial solvent [11].

It is well known that chemocatalysts can effectively facilitate the transformation of lignocellulosic biomass into furfural within suitable solvent systems [12–14]. Although water is often suggested as the most eco-friendly reagent, furfural production can be hindered in the single water system due to the poor solubility of furfural [15]. However, furfural is easy to dissolve in some organic solvents. The constructed organic solvent–water system facilitates the furfural generation, and the formed furfural can be extracted into the organic phase, avoiding its degradation during the transformation of biomass into furfural [16,17]. Accordingly, an attempt is needed to establish an organic solvent–H<sub>2</sub>O reaction medium for

converting biomass into furfural. Currently, many organic solvents (e.g., methyl isobutyl ketone (MIBK),  $\gamma$ -valerolactone (GVL), and cyclopentyl methyl ether (CPME)) have been utilized to acquire furfural from biomass or biomass-derived *D*-xylose [18–21]. It is known that CPME is a green and effectual organic solvent. In a CPME-H<sub>2</sub>O mixture (1:1, *v/v*), birch-hydrolysate was transformed into furfural in 68% yield at 190 °C [16].

Industrially, conventional homogeneous acids (H<sub>2</sub>SO<sub>4</sub> and HCl) are commonly utilized as chemocatalysts for preparing furfural [22], which are prone to causing equipment corrosion, environmental pollution, and product recovery difficulties. On the contrary, heterogeneous biochar-based chemocatalysts have properties of low corrosion, good chemocatalytic selectivity, excellent thermostability, and easy separation [23]. As green chemocatalysts, biochar-based solid acid chemocatalysts have attracted more and more researchers' attention [24,25]. Gong et al. prepared a biochar-based chemocatalyst SO<sub>4</sub><sup>2-</sup>/SnO<sub>2</sub>-SSXR for transforming xylose-rich hydrolysates into furfural in a yield of 83% in a choline chloride-maleic acid-toluene mixture [12]. Dai et al. prepared biochar-based solid acid S-IRCC to transform *D*-xylose into furfural in a 74% yield in a MIBK-H<sub>2</sub>O (2:1, *v:v*) mixture containing NaCl (60 g/L) at 190 °C within 1 h [18].

As is well known, hulls are the outermost layers of wheat grains, and barley hulls (BHs) account for 15–20% of the dry weight of grains. The global annual output of barley is around 146 million tons. Accordingly, the effectual utilization of BH resources has gained much attention. However, to date, there are few works on the synthesis of BH-based heterogeneous chemocatalysts for effectual transformation of biomass into furfural in eco-friendly reaction systems. As one of the biological wastes, BH has a unique chemical composition and structural properties [26]. In this research, the merits of a heterogeneous chemocatalyst and a green solvent system were combined. A new tin-based biochar heterogeneous chemocatalyst Sn-NUS-BH was acquired using BH as support, and furfural was acquired through the catalysis of corncob in a CPME-H<sub>2</sub>O reaction system. The influences of reaction duration, performance temperature, Sn-NUS-BH dose, solvent type and dosage, metal chloride salt type, and ZnCl<sub>2</sub> loading on the corncob conversion to furfural were tested. An effectual CPME-H<sub>2</sub>O reaction system containing Sn-NUS-BH was built for the conversion of corncob into furfural, which afforded a promising process for the valorization of biomass.

## 2. Results and Discussion

### 2.1. Characteristics of Sn-NUS-BH

The tin-based sulfonated biochar Sn-NUS-BH chemocatalyst was created using a series of operation steps. The pore structure and surface characteristics of NaOH-ultrasonic-treated BH (NUS-BH) and chemocatalyst Sn-NUS-BH were measured using the BET method. In Table 1, Sn-NUS-BH had an increased specific surface area (63.2 m<sup>2</sup>/g), an augmented pore volume (0.15 cm<sup>3</sup>/g), and a declined pore size (2.8 nm). In the preparation of Sn-NUS-BH, protein and other components in BH were removed by an alkali solution (0.5 M NaOH) combined with an ultrasonic treatment (100 W, 50 °C). Solvents (e.g., H<sub>2</sub>SO<sub>4</sub>, ammonia water, and ethanol) and calcining (550 °C) made the NUS-BH structure slack and tight, thus augmenting specific surface area, enlarging pore volume, and decreasing pore size. The alterations might have had a crucial effect on the chemocatalytic activity of heterogeneous chemocatalysts [27], which facilitated additional loading of Sn<sup>4+</sup> ions and sulfonic acid groups on Sn-NUS-BH. The smaller pore size might block more Sn<sup>4+</sup> ions, which would enhance the chemocatalytic activity of solid acid [28].

**Table 1.** Structural analysis of NUS-BH and solid acid Sn-NUS-BH.

Sample	Specific Surface Area, m <sup>2</sup> /g	Pore Volume, cm <sup>3</sup> /g	Pore Size, nm
NUS-BH	0.6	0.04	11.8
Sn-NUS-BH	63.2	0.15	2.8

SEM was applied to observe the surface morphology changes in NUS-BH and Sn-NUS-BH (Figure 1). The NUS-BH surface was smooth, while the Sn-NUS-BH surface was rough and porous, which was consistent with the results of the augmented specific surface area, enlarged pore volume, and decreased pore size (Table 1). These alterations facilitated the loading of sulfonic acid groups (Brønsted acid sites) on Sn-NUS-BH. Some tiny particles might attach to the surface of Sn-NUS-BH, which helped SnO<sub>2</sub> (Lewis acid site) generate covalent bonds with carbon groups [29]. Brønsted and Lewis acids with strong acidity might attach to the Sn-NUS-BH surface. When the Sn-NUS-BH was entirely in contact with corncob powders, the chemocatalytic efficiency improved.

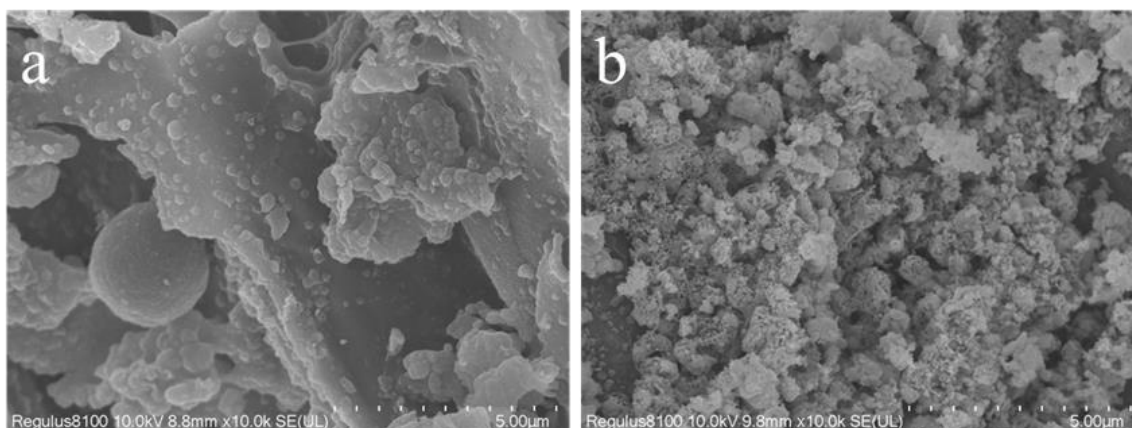


**Figure 1.** SEM characterization of NUS-BH (a) and Sn-NUS-BH solid acid catalyst (b).

XRD was applied to visualize the crystal structure of NUS-BH and Sn-NUS-BH (Figure 2). They had apparent characteristic peaks at 26.5°, which corresponded to the crystal structure of carbon. Through the sulfonation, the peak width of Sn-NUS-BH arose at the crystal plane of carbon, verifying that the sulfonic acid group might connect to the abnormal carbon structure. The peaks near 33.8° and 51.9° were ascribed to the tin ion, which might be adequately loaded on the Sn-NUS-BH, leading to a solid crystal structure occurring [13,28]. By comparing NUS-BH and Sn-NUS-BH, the position of abscissa was fundamentally unchanged, testifying that the basic structure of the BH shell was not substantially damaged before and after treatment.

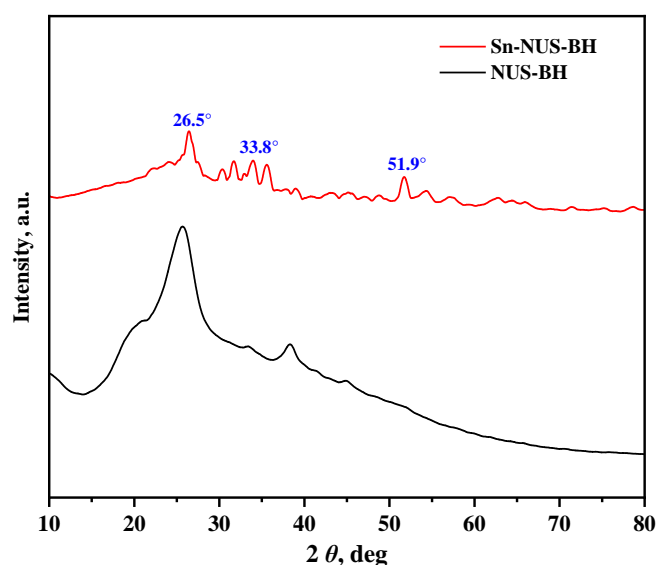


**Figure 2.** XRD images of NUS-BH and solid acid Sn-NUS-BH.

FT-IR was used to characterize NUS-BH and Sn-NUS-BH (Figure 3). The peak around  $3435\text{ cm}^{-1}$  originated from the stretching vibration of O-H groups [30]. The peak near  $2826\text{ cm}^{-1}$  was related to the stretching vibration of C-H. The existence of Brønsted acid sites on Sn-NUS-BH was attributed to a wavelength of  $1640\text{ cm}^{-1}$  [31]. The peaks near  $1116\text{ cm}^{-1}$  and  $778\text{ cm}^{-1}$  were associated with  $\text{Sn}^{4+}$  and  $\text{SO}_4^{2-}$  on the surface of Sn-NUS-BH, and O=S=O stretching was observed, implying the loading of sulfonic groups as Brønsted acid sites on Sn-NUS-BH [28]. The peak around  $622\text{ cm}^{-1}$  was associated with  $\text{SnO}_2$  as Lewis acid sites [30,32], confirming that  $\text{Sn}^{4+}$  ions were loaded on NUS-BH.

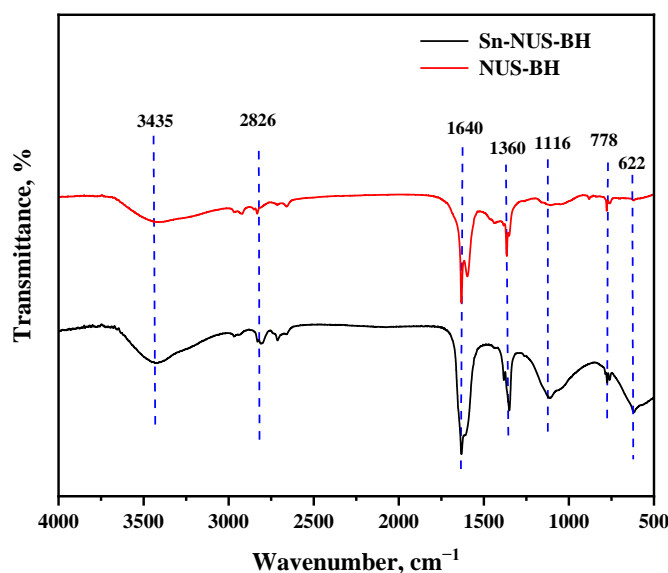


Figure 3. Infrared characterization of NUS-BH and solid acid Sn-NUS-BH.

The valence state of the Sn element on Sn-NUS-BH could be measured through an XPS analysis (Figure 4). Three valence states of tin ions (0, +2, and +4) were observed. It was found that the contents of  $\text{Sn}^03d_{5/2}$ ,  $\text{Sn}^{2+}3d_{5/2}$ , and  $\text{Sn}^{4+}3d_{5/2}$  were 14.38%, 48.95%, and 36.67%, respectively. In the preparation of Sn-NUS-BH, tin ions with +4 valence formed. Additionally,  $\text{SnO}_2$  might enhance the hydrolysis of xylan to *D*-xylose and accelerate the dehydration of *D*-xylose into furfural [3].

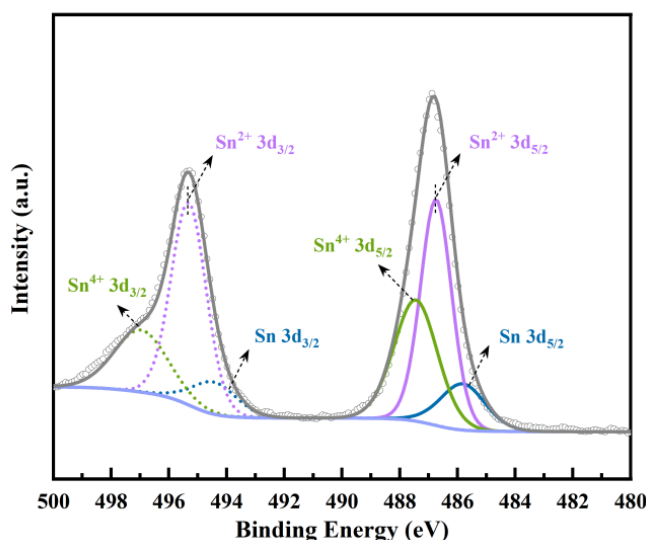


Figure 4. XPS characterization of NUS-BH and solid acid Sn-NUS-BH. [Gray line, sum of all deconvolution curves; light purple lines, background curve].

According to the analysis with the temperature-programmed desorption (TPD) with  $\text{NH}_3$ , the acid sites on Sn-NUS-BH were measured. Generally, strong (400–800 °C), medium (200–400 °C), and weak (100–200 °C) acid sites may be determined [13,33]. As showcased in Figure 5, Sn-NUS-BH had two strong acid sites at 750 and 800 °C. The strong acid sites had a crucial role in the hydrolysis and dehydration reaction, which favored the hydrolysis of xylan in biomass into *D*-xylose and further dehydration of *D*-xylose to furfural [34].

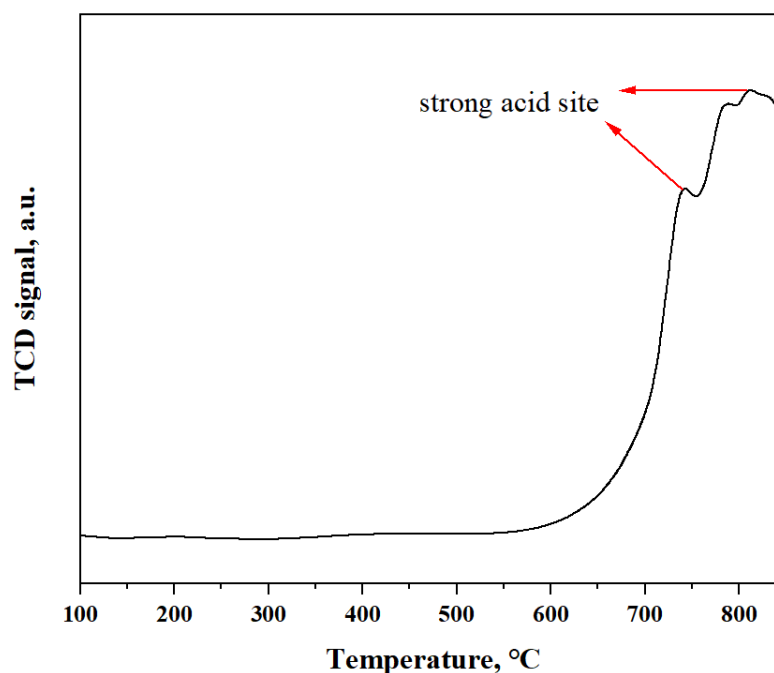
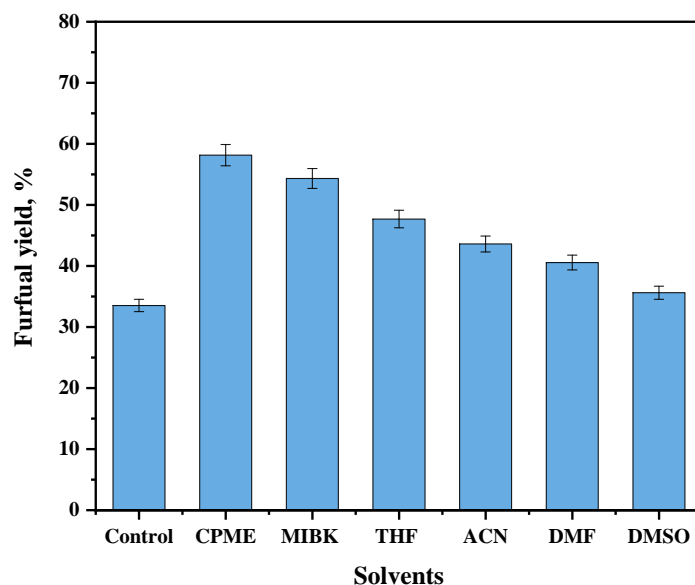


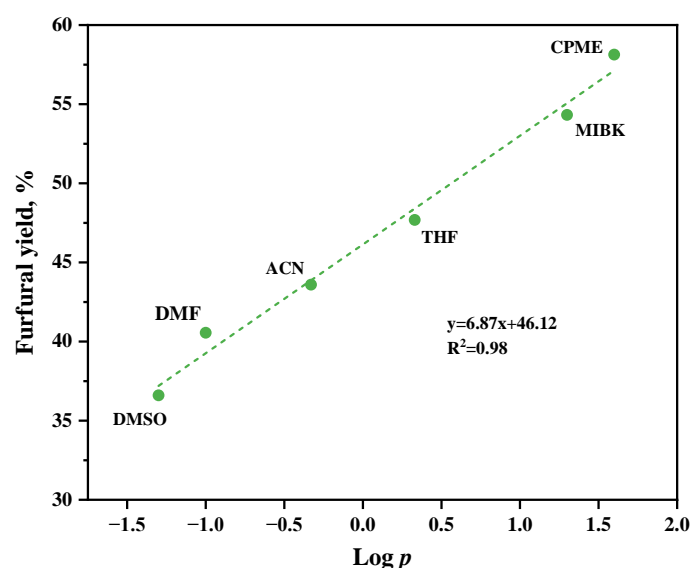
Figure 5.  $\text{NH}_3$ -TPD characterization of NUS-BH and Sn-NUS-BH solid acid catalysts.

### 2.2. Effect of Organic Solvents on Furfural Yield

It is known that the solubility of furfural is poor in a single water system, so the transformation of biomass into furfural would be restricted during the preparation of furfural. Different from the single aqueous phase, the merit of an organic solvent–water reaction system is that the generated furfural can be rapidly extracted into the organic phase [35]. Utilizing an organic solvent–water reaction system not only avoids the tedious steps of collecting furfural but also alleviates the generation of by-products [12]. To examine the chemocatalytic performance of Sn-NUS-BH in different organic solvent–water media, six organic solvents, including CPME, MIBK, GVL, THF, DMF, and DMSO, were separately supplemented into the aqueous system to promote furfural generation (Figure 6a). The results showcased that the yield of furfural in CPME- $\text{H}_2\text{O}$  reached the highest amount (58.1%), which was 1.73 times higher than that in the single water system. For other organic solvents, the furfural yields were relatively low, which were ascribed to the fact that the most suitable organic solvents might be different in the different reaction media. In previous studies, furfural was synthesized from carbohydrates in biomass in butanone water, reaching a yield of 56% [36]. As the organic solvent was mixed with water, the hydrogen bond and polarity of the solvent were altered, thus influencing the thermodynamics of the *D*-xylose dehydration reaction. Figure 6b showcases the relationship of the oil–water partition coefficient ( $\text{Log } P$ ) of organic solvents in the reaction system and the corresponding furfural yield. It could be interpreted that  $\text{Log } P$  was linearly related to the yield of furfural. A high  $\text{Log } P$  of solvent could favor the furfural generation, and CPME with the highest  $\text{Log } P$  could give the maximum furfural yield.



(a)



(b)

**Figure 6.** The effect of five organic solvents (CPME, MIBK, THF, ACN, DMF, and DMSO) on furfural yield [corn cob 3 g (75 g/L), organic solvent/water = 1:1 (v/v), Sn-NUS-BH 3.6 wt%, 170 °C, 20 min] (a); The relationship between furfural yield and organic solvent log  $P$  [corn cob 3 g (75 g/L), organic solvent/water = 1:1 (v/v), Sn-NUS-BH 3.6 wt%, 170 °C, 20 min] (b).

As showcased in Figure 7, upon increasing the ratio of CPME-to-water from 1:3 to 2:1 (v/v), a sharp increase in furfural yield was observed. With a decreasing water ratio in the reaction system, the *D*-xylose dehydration ability was increased. The generated furfural could be extracted into the CPME phase, and the potential furfural degradation was weakened. Upon raising the volumetric ratio of CPME-to-H<sub>2</sub>O from 2:1 to 3:1, a slight increase in furfural yield was observed. Thus, the optimum CPME-to-H<sub>2</sub>O ratio was 2:1 (v/v). In the previous work, furfural was acquired from *D*-xylose by sulfonation-functionalized metal-organic frameworks MIL-101(Cr)-SO<sub>3</sub>H, and the yield of furfural reached 70.8% in CPME–water (mass ratio, 2:1), while furfural was acquired in the yield

of 50.5% in an aqueous solution [37]. The supplementation of CPME into water to form the CPME–water reaction system substantially promoted the formation of furfural. Accordingly, the appropriate volumetric ratio of CPME-to-water was 2:1 in this research. The proper supplementation of CPME might favor the extraction of furfural and increase the chemocatalytic activity of Sn-NUS-BH, enabling the formed CPME–water system to reduce the decomposition of furfural and improve furfural yield.

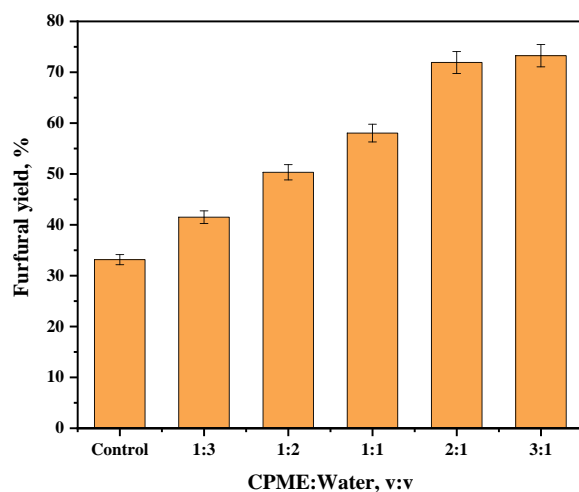


**Figure 7.** The effect of the volumetric ratio of CPME-to-water (1:3–3:1,  $v/v$ ) on the formation of furfural [corncob 3 g (75 g/L), Sn-NUS-BH 3.6 wt%, 170 °C, 20 min].

### 2.3. Synthesis of Furfural from Corncob by Sn-NUS-BH in CPME–Water Two-Phase System

Distinct from homogeneous catalysts, heterogeneous catalysts have been extensively utilized and studied due to their advantages of low-performance cost, high chemocatalytic activity, and good reusability [38]. Different from the single water system, the merit of a CPME–H<sub>2</sub>O two-phase system was that it might rapidly extract furfural into the organic phase CPME and decline the furfural decomposition, avoiding the generation of by-products. To examine the influence of other factors on the synthesis of furfural from corncob through the catalysis with Sn-NUS-BH in CPME–H<sub>2</sub>O (2:1,  $v/v$ ), the Sn-NUS-BH dose (0–6.0 wt%), reaction duration (5–60 min), and catalytic temperature (150–190 °C) were optimized (Figures 8 and 9).

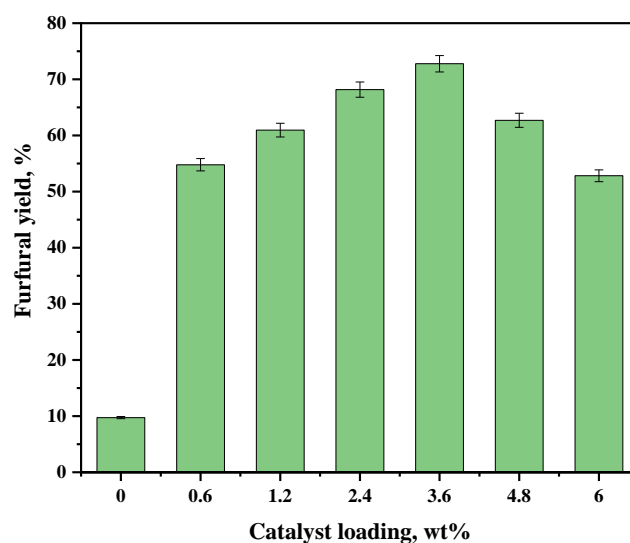


**Figure 8.** Effect of Sn-NUS-BH (0–6 wt%) on the catalytic conversion of corncob to furfural under 170 °C for 20 min in CPME–water (2:1,  $v/v$ ) system.

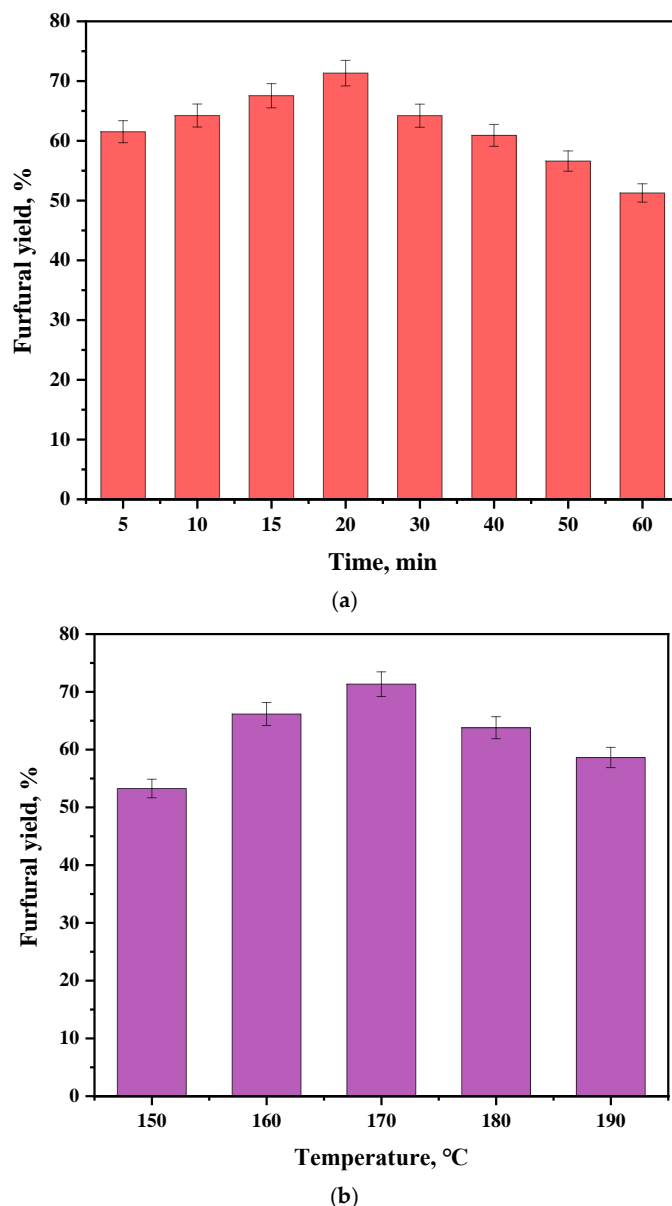


**Figure 9.** Effects of reaction time (5–60 min) on the chemocatalysis of corncob into furfural with Sn-NUS-BH (3.6 wt%) at 170 °C in CPME–water (2:1, *v/v*) (a); effects of temperature (150–190 °C) on the chemocatalysis of corncob into furfural with Sn-NUS-BH (3.6 wt%) at 170 °C for 20 min in CPME–water (2:1, *v/v*) (b).

As the Sn-NUS-BH dose rose from 0.6 to 3.6 wt%, the furfural yield gradually elevated (Figure 8). When Sn-NUS-BH was 3.6 wt%, the yield of furfural reached the maximum. With increasing the dosage of Sn-NUS-BH, the number of acid-catalyzed sites and the acidity increased, which would promote furfural generation. However, an excessive increase in Sn-NUS-BH resulted in unwanted side reactions, which might reduce the furfural yield. Thus, 3.6% was selected as the suitable Sn-NUS-BH loading. Under these conditions, the effects of reaction duration (5–60 min) and performance temperature (150–190 °C) on furfural generation were studied (Figure 9a,b). In 20 min, the yield of furfural reached its highest level (71.4%). As showcased in Figure 9b, the furfural yield was 71.4% at 170 °C in 20 min, and the yield of furfural gradually declined with increasing reaction temperature. Elevated temperatures might not only promote furfural formation but also aggravate some unwanted high-temperature side reactions. The by-products might attach to the Sn-NUS-

BH active sites, which would weaken the chemocatalytic activity and decline the yield of furfural [39].

Studies have shown that adding chloride salts in the process of furfural synthesis might stabilize the structure of the transition and states and weaken undesirable side reactions, which leads to increased furfural yield [40]. To explore the influences of chlorides on the catalytic activity of furfural catalyzed by Sn-NUS-BH, twelve chloride salts were individually added into reaction media in order to test the changes in furfural yield. As showcased in Figure 10a, NaCl, BaCl<sub>2</sub>, MnCl<sub>2</sub>, NiCl<sub>2</sub>, CuCl<sub>2</sub>, SnCl<sub>4</sub>, and CrCl<sub>3</sub> might inhibit the generation of furfural in CPME–water. AlCl<sub>3</sub> had no substantial inhibitory effect on the production of furfural, while ZnCl<sub>2</sub>, FeCl<sub>3</sub>, MgCl<sub>2</sub>, and CaCl<sub>2</sub> could promote the formation of furfural in CPME–water. Notably, ZnCl<sub>2</sub> (50 mM) had a pronounced increase in the yield of furfural, reaching 80.5%. Considering the positive role of ZnCl<sub>2</sub> in the reaction system, diverse doses of ZnCl<sub>2</sub> (0–500 mM) were individually added into the CPME–H<sub>2</sub>O system to examine its influence on the chemocatalytic activity of Sn-NUS-BH (Figure 10b). At a concentration of 50 mM ZnCl<sub>2</sub>, the yield of furfural reached the highest level (80.5% yield). The supplementation of ZnCl<sub>2</sub> could effectually promote the production of furfural from corncob. ZnCl<sub>2</sub> might participate in the pyrolysis reaction by coordinating with the O atom of *D*-xylose. The *D*-xylose–ZnCl<sub>2</sub> complexes that coordinated with two O atoms are usually more stable than those combined with a single O atom. Through the chemocatalysis with ZnCl<sub>2</sub>, the acyclic *D*-xylose degradation channel is more conducive to the formation of furfural and lowers the activation-free energy [41]. Additionally, ZnCl<sub>2</sub> might have a positive role in the depolymerization of xylan chains to selectively form furfural by promoting the hydrolysis of glycosidic bonds. In this work, untreated corncob was composed of 36.5% glucan, 32.6% xylan, and 17.8% lignin. When added to CPME–water, Sn-NUS-BH can dehydrate *D*-xylose to form furfural, while glucan is generally transformed into 5-HMF and levulinic acid. It was found that Sn-NUS-BH and ZnCl<sub>2</sub> could hydrolyze glucan and xylan, resulting in the dehydration of furan compounds (HMF and furfural) and levulinic acid in CPME–H<sub>2</sub>O.

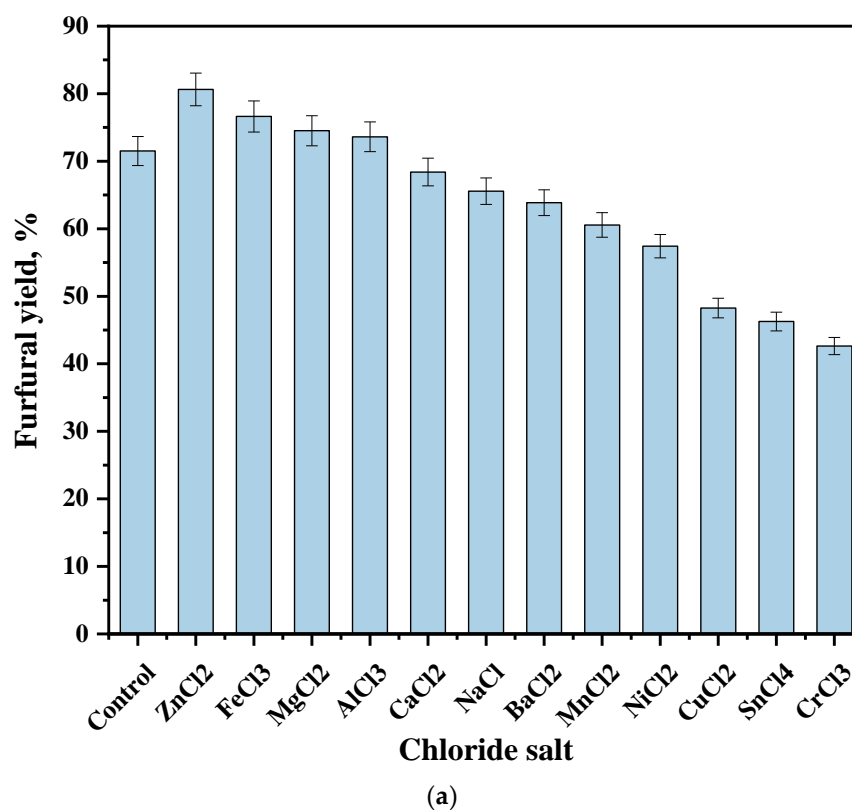
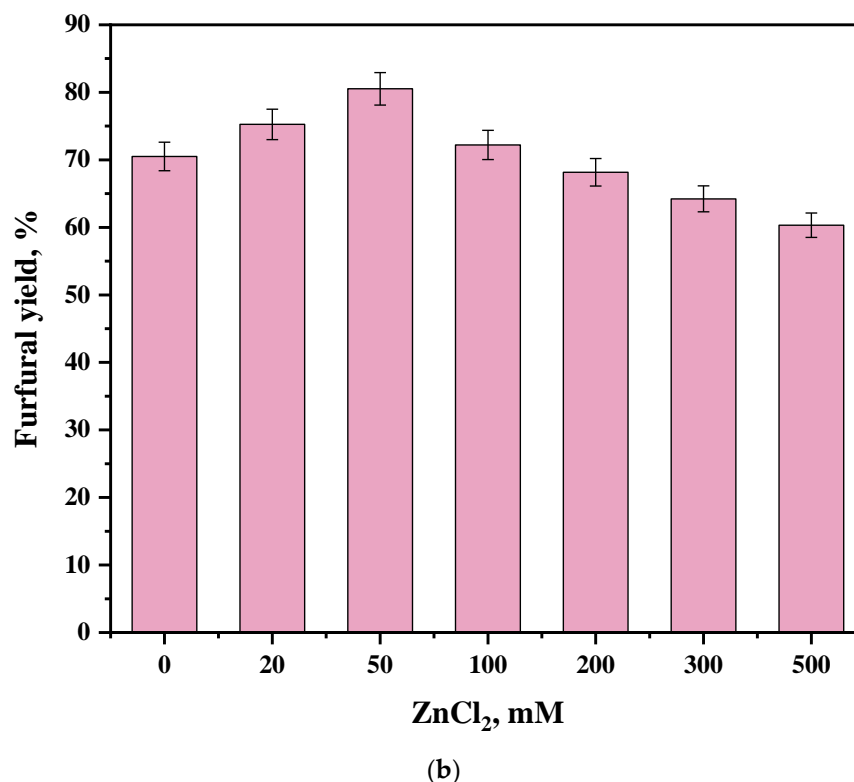


Figure 10. Cont.



**Figure 10.** Effects of chloride salts (50 mM) on the chemocatalysis of corncob into furfural with Sn-NUS-BH (3.6 wt%) at 170 °C for 20 min in CPME–water (2:1, *v/v*) (a); effects of ZnCl<sub>2</sub> dosage (0–500 mM) on the chemocatalysis of corncob into furfural with Sn-NUS-BH (3.6 wt%) at 170 °C for 20 min in CPME–water (2:1, *v/v*) (b).

In industrial applications, heterogeneous chemocatalysts are often recycled many times due to their advantages of easy recycling and good reusability [42]. To assess the performance stability of Sn-NUS-BH in CPME–H<sub>2</sub>O, six recycling experiments were conducted under the acquired optimum reaction conditions. After each reuse, Sn-NUS-BH was recovered by filtration, water washed, oven-dried (80 °C) for 12 h, and calcined (550 °C) for 4 h, and then the chemocatalytic reaction was conducted after calcination. As showcased in Figure 11, from the first batch to the sixth batch, the yield of furfural declined from 80.5% to 65.7%, which might be ascribed to the gradual loss of tin ions from Sn-NUS-BH with repeated recycling. The active sites and void structures on Sn-NUS-BH were blocked and covered by some impurities in the catalysis process, which led to reduced chemocatalytic activity. Sn-NUS-BH was reused six times, and the yield of furfural weakened by 14.4%. The solid acid SC-FAR-800 was reused six times, and the yield of furfural declined from 60.6% (the first batch) to 30.3% (the sixth batch) [43]. These results displayed that Sn-NUS-BH had good reusability and excellent thermostability, and the good recyclability and reusability of Sn-NUS-BH would effectually decrease the production cost.

It is well-known that biomass extensively serves as an abundant, low-cost, easily obtained, and renewable bioresource for the production of value-added biobased compounds and functional materials [44–48]. Utilizing barley hull (BH) as biobased support, the sulfonated tin-based heterogeneous catalyst Sn-NUS-BH was synthesized. CPME–H<sub>2</sub>O (2:1, *v/v*) was utilized as an environmentally friendly reaction medium for the transformation of corncob into furfural, which would avoid the undesired side-reactions, enhance the chemocatalytic effect of Sn-NUS-BH, and promote the furfural productivity, realizing the green and sustainable production of furfural. Distinct from the used carrier NUS-BH, the prepared chemocatalyst Sn-NUS-BH had a larger relative surface area and pore volume, which could support more SnO<sub>2</sub> (Lewis acid site) and sulfonic acid groups (Brønsted acid site). These catalytic sites on solid acid had a high selectivity for transforming hemicellulose

in lignocellulose into furfural. The surface of NUS-BH was rough and porous with a special circular pore structure. More tin ions and  $-\text{SO}_3\text{H}$  groups were loaded on Sn-NUS-BH to generate highly uniform chemocatalytic active sites (Lewis/Brønsted acid sites). The transformation of lignocellulose into furfural was carried out via synergistic catalysis of Brønsted/Lewis acid sites on Sn-NUS-BH. Brønsted acids transformed the depolymerization of xylan into xylose, and the formed *D*-xylose was subsequently isomerized into xylulose with Lewis acids, and eventually, Brønsted acids catalyzed the dehydration of xylulose to furfural [39,42]. CPME might alter the dense structure of lignocellulose and disrupt the physical and chemical connections among biomacromolecules (e.g., hemicellulose, lignin, and cellulose), thereby depolymerizing and hydrolyzing hemicellulose. At high temperatures, the metal cation  $\text{ZnCl}_2$  and CPME broke the intramolecular hydrogen bonds that existed between lignin and hemicellulose.  $\text{Cl}^-$  could form hydrogen bonds with the O-H groups of hemicellulose and lignin [12]. The  $\beta$ -1,4-glycosidic bonds in carbohydrates (hemicellulose plus cellulose) were disrupted by protons on Sn-NUS-BH. Xylan in the corncob could be hydrolyzed into *D*-xylose in CPME–water.  $\text{ZnCl}_2$  could be used as a Lewis acid catalyst.  $\text{Zn}^{2+}$  might favor the isomerization of *D*-xylose into xylulose, which then eliminated three molecules of  $\text{H}_2\text{O}$  to generate furfural. The supplementation of  $\text{ZnCl}_2$  enhanced the interaction between CPME and Sn-NUS-BH. These synergies could promote furfural production through the enhancement of *D*-xylose isomerization and xylulose dehydration. This constructed sustainable process manifested high potential application for furfural production from biomass with a biobased chemocatalyst in a benign reaction medium. In a concise summary, a substantial improvement in furfural production from lignocellulose with biobased chemocatalyst Sn-NUS-BH was successfully realized in CPME–water containing  $\text{ZnCl}_2$ .

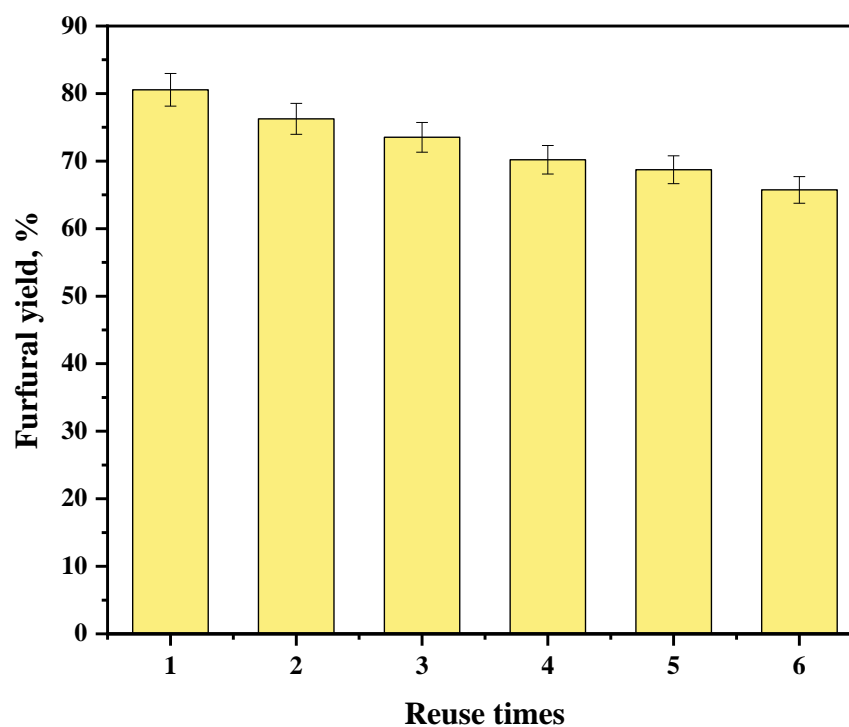


**Figure 11.** Recycling of Sn-NUS-BH for converting corncob into furfural at 170 °C for 20 min in CPME–water (2:1, *v/v*) containing  $\text{ZnCl}_2$  (50 mM).

### 3. Materials and Methods

#### 3.1. Chemicals and Materials

Corncob, which was composed of 36.5% glucan, 32.6% xylan, and 17.8% lignin, was harvested from a farm in Zhoukou (Henan Province, China). Barley hulls (BHs) were

collected from a brewery in Hangzhou (Zhejiang Province, China) and were composed of 18.5% glucan, 23.7% xylan, and 18.1% lignin. Cyclopentyl methyl ether (CPME), methyl isobutyl ketone (MIBK), tetrahydrofuran (THF), acetonitrile (ACN), dimethyl sulfoxide (DMSO), *N,N*-dimethylformamide (DMF), and other chemicals used in this research were from Sinopharm Group Chemical Reagent Co., Ltd. (Shanghai, China).

### 3.2. Preparation of Solid Acid Sn-NUS-BH

BHs were ground with a grinder (SUS 304, Hefei Rongzhida Sanyo Electric Co., Ltd., Hefei, China) to acquire 40–60 mesh of BH powder (0.2 kg). The powders were soaked in 800 mL ethanol solution containing NaOH (0.50 M) in an ultrasonic instrument (KH2200B, Kunshan Hechuang Ultrasonic Instrument Co., Ltd., Kunshan, China) (100 W, 50 °C) for 240 min. The NaOH-ultrasonic-treated BH (NUS-BH) was then filtered, separated, and rinsed with distilled water until neutral. After drying over an oven (60 °C), the acquired NUS-BH was mixed with 0.10 kg glucose in 500 mL distilled water and then treated ultrasonically for 60 min. Afterward, the mixture was filtered and oven-dried. The dried powders were calcined in a Muffle furnace (550 °C, 240 min). The resulting slurry was mixed with 600 mL ethanol and 40.0 g SnCl<sub>4</sub>·5H<sub>2</sub>O, and the pH of this mixture was regulated to 6.0 with ammonia (25.0 wt%). The resulting colloidal solution was oven-dried (80 °C, 48 h). The resulting dried powder was soaked in 4.0 M H<sub>2</sub>SO<sub>4</sub> at 60 °C. After 4 h of sulfonation, the sulfonated solid powders were filtered and further oven-dried (80 °C). Afterward, the resulting black powders were calcined (550 °C). After 240 min, the formed Sn-NUS-BH catalyst was further applied to transform biomass into furfural.

### 3.3. Chemical Transformation of Corncob into Furfural by Sn-NUS-BH in Organic Solvent–Water System

Next, 40 mL organic solvation–water mixture was mixed with 3.0 g dried and milled corncob powders (~40 mesh) and a certain amount of Sn-NUS-BH in a 100 mL Jqf0002 stainless-steel autoclave (Suzhou Shenghua Instrument Technology Co., Ltd., Suzhou, China) by magnetic stirring (550 rpm) to produce furfural at the designed reaction temperature for the designed reaction time. Several chemical reaction factors influencing the formation of furfural were tested, including different organic solvent types (CPME, THF, ACN, MIBK, DMSO or DMF), the volumetric ratio of organic solvent to water (1:3, 1:2, 1:1, 2:1 or 3:1, *v/v*; pH 1.5), Sn-NUS-BH load (0.6, 1.2, 2.4, 3.6, 4.8 or 6.0 wt%), performance temperature (150, 160, 170 or 180 °C), and reaction duration (10, 15, 20, 30, 40 or 50 min). The effects of metal chloride salts and zinc ion dose (0, 20, 50, 100, 200, 300, or 500 mM) were explored on the furfural formation in CPME–water (2:1, *v/v*, 170 °C). After 20 min, furfural was quantified with HPLC. LogR<sub>0</sub> was used to assess the influence of different reaction temperatures and reaction durations during the chemical reaction process. The below equation was calculated from reaction time (*t*, min) and reaction temperature (*T*, °C).

$$\text{Log}R_0 = \text{Log}\left(t \times \exp\frac{T - 100}{14.75}\right) \quad (1)$$

### 3.4. Reuse of Sn-NUS-BH

To assess the reusability and thermostability of Sn-NUS-BH, the recovered Sn-NUS-BH was reused six times to catalyze the transformation of corncob into furfural. After each use, Sn-NUS-BH was recovered by simple filtration, entirely washed with DI water, oven-dried (80 °C), and then Muffle furnace-calcined (550 °C) to eliminate residue from the Sn-NUS-BH surface. The recovered Sn-NUS-BH was used in the next batch of reactions. Each batch of samples was reacted in a 40 mL CPME–H<sub>2</sub>O (2:1, *v/v*) mixture composed of 75 g/L corncob and 50 mM ZnCl<sub>2</sub> by autoclaving at 170 °C for 20 min.

### 3.5. Structural Features of Corncob and Sn-NUS-BH

The structures of the corncob and Sn-NUS-BH surface were characterized by SEM (Regulus 8100, Hitachi, Tokyo, Japan), FT-IR (Nicolet iS50, Thermo, Madison, WI, USA),

XRD (D/MAX-2500; Rigaku, Tokyo, Japan). The accessibility of corncob was assessed through the dye adsorption of Congo red dye [49]. BET (Autosorb-IQ2-MP, Quanta chrome, Boynton Beach, FL, USA) surface area obtained via N<sub>2</sub> adsorption was adopted to characterize surface area/pore size/pore volume for NUS-BH and Sn-NUS-BH. The specific surface area of the sample was analyzed based on the N<sub>2</sub> adsorption isotherm; the pore structure of the sample, including pore volume and pore diameter, was analyzed based on the single-point adsorption of N<sub>2</sub>. NH<sub>3</sub>-TPD was implemented by using a BELCAT II chemisorption system (BELCAT II, MicrotracBEL, Osaka, Japan) to measure the acid strength of Sn-NUS-BH. Sn-NUS-BH (100 mg) was treated for 60 min with a helium atmosphere (300 °C). The sample was then cooled down to 50 °C. After adsorption of NH<sub>3</sub> at 50 °C for 60 min, Sn-NUS-BH was pretreated with helium to remove excessive NH<sub>3</sub> and then heated to 850 °C for NH<sub>3</sub> desorption at a flow rate of 30–50 mL per minute and a heating rate of 10 °C per minute. The desorption gas was detected by TCD.

#### 4. Conclusions

A biochar-based chemocatalyst, Sn-NUS-BH, was synthesized using BH as a carrier and applied for the transformation of corncob into furfural in a CPME-H<sub>2</sub>O (2:1, *v/v*) system containing ZnCl<sub>2</sub> (50 mM) at 170 °C for 20 min, achieving a high furfural yield of 80.5%. Sn-NUS-BH demonstrated excellent thermal stability and reusability, maintaining its catalytic efficiency over six cycles. This study presents an eco-friendly and efficient process for the conversion of biomass into furfural using Sn-NUS-BH in a CPME-H<sub>2</sub>O system, offering significant potential for the sustainable production of valuable biobased chemicals from lignocellulosic biomass.

**Author Contributions:** Conceptualization, methodology, software, validation, formal analysis, investigation, sources, data curation, and writing—original draft: B.F. and L.K.; supervision, writing—review, and editing: Y.H. All authors have read and agreed to the published version of the manuscript.

**Funding:** This research received no external funding.

**Institutional Review Board Statement:** Not applicable.

**Data Availability Statement:** Data are contained within this article.

**Acknowledgments:** The authors thank the Analysis and Testing Center (Changzhou University) for the analysis of samples with SEM, FT-IR, and XRD. All individuals included in this section have consented to the acknowledgement.

**Conflicts of Interest:** The authors declare no conflict of interest to this research, and this paper has not been submitted to any other journal simultaneously.

#### References

1. Mao, G.; Liu, X.; Du, H.; Zuo, J.; Wang, L. Way forward for alternative energy research: A bibliometric analysis during 1994–2013. *Renew. Sustain. Energy Rev.* **2015**, *48*, 276–286. [[CrossRef](#)]
2. Fernandez, M.L.; Len, T.; Urbanob, J.; Balu, A.; Luque, R. Transformation of furfural into dimorpholinocyclopentenone using Al-SBA-15 materials. *Sustain. Chem. Pharm.* **2024**, *39*, 101573. [[CrossRef](#)]
3. He, Y.-C.; Jiang, C.-X.; Chong, G.-G.; Di, J.-H.; Wu, Y.-F.; Wang, B.-Q.; Xue, X.-X.; Ma, C.-L. Chemical-enzymatic conversion of corncob-derived xylose to furfuralcohol by the tandem catalysis with SO<sub>4</sub><sup>2-</sup>/SnO<sub>2</sub>-kaoline and *E. coli* CCZU-T15 cells in toluene–water media. *Bioresour. Technol.* **2017**, *245*, 841–849. [[PubMed](#)]
4. Hu, S.L.; Liang, S.; Mo, L.Z.; Su, H.H.; Huang, J.S.; Zhang, P.J.; Qi, J.N. Conversion of biomass-derived monosaccharide into furfural over Cr–Mg-LDO@bagasse catalysts. *Sustain. Chem. Pharm.* **2023**, *32*, 101013. [[CrossRef](#)]
5. Licursi, D.; Galletti, M.R.; Bertini, B.; Ardemani, L.; Scotti, N.; Fidio, N.D.; Fulignati, S.; Antonetti, C. Design approach for the sustainable synthesis of sulfonated biomass-derived hydrochars and pyrochars for the production of 5-(hydroxymethyl)furfural. *Sustain. Chem. Pharm.* **2023**, *39*, 101573. [[CrossRef](#)]
6. Lu, Y.; He, Q.; Fan, G.; Cheng, Q.; Song, G. Extraction and modification of hemicellulose from lignocellulosic biomass: A review. *Green Process. Synth.* **2021**, *10*, 779–804. [[CrossRef](#)]
7. Yatis, R.G.; Kumar, D.H.; Chinnabhandar, R.K.; Raviraj, H.M.; Ravi Shankar, A.U. A review of the potential application of lignin in the production of bio-binder: Challenges and opportunities. *J. Mater. Sci.* **2024**, *59*, 3205–3224.

8. Terrett, O.M.; Dupree, P. Covalent interactions between lignin and hemicelluloses in plant secondary cell walls. *Curr. Opin. Biotechnol.* **2019**, *56*, 97–104. [[CrossRef](#)]
9. Liu, C.; Wei, L.; Yin, X.; Wei, M.; Xu, J.; Jiang, J.; Wang, K. Selective conversion of hemicellulose into furfural over low-cost metal salts in a  $\gamma$ -valerolactone/water solution. *Ind. Crops Prod.* **2020**, *147*, 112248. [[CrossRef](#)]
10. Wang, Y.; Lu, J.; Zhou, S.; Du, J.; Tao, Y.; Cheng, Y.; Wang, H. Bioconversion of cellulose and hemicellulose in reed sawdust to xylo-oligosaccharides and L-lactic acid. *Ind. Crops Prod.* **2022**, *187*, 115390. [[CrossRef](#)]
11. Wang, Z.; Bhattacharyya, S.; Vlachos, D.G. Extraction of furfural and furfural/5-hydroxymethylfurfural from mixed lignocellulosic biomass-derived feedstocks. *ACS Sustain. Chem. Eng.* **2021**, *9*, 7489–7498. [[CrossRef](#)]
12. Gong, L.; Zha, J.; Pan, L.; Ma, C.; He, Y.C. Highly efficient conversion of sunflower stalk-hydrolysate to furfural by sunflower stalk residue-derived carbonaceous solid acid in deep eutectic solvent/organic solvent system. *Bioresour. Technol.* **2022**, *351*, 126945. [[CrossRef](#)] [[PubMed](#)]
13. Shen, J.; Gao, R.; He, Y.-C.; Ma, C. Efficient synthesis of furfural from waste biomasses by sulfonated crab shell-based solid acid in a sustainable approach. *Ind. Crops Prod.* **2023**, *202*, 116989. [[CrossRef](#)]
14. Yang, Q.; Tang, W.; Ma, C.; He, Y.C. Efficient co-production of xylooligosaccharides, furfural and reducing sugars from yellow bamboo via the pretreatment with biochar-based catalyst. *Bioresour. Technol.* **2023**, *387*, 129637. [[CrossRef](#)]
15. Sato, O.; Mimura, N.; Masuda, Y.; Shirai, M.; Yamaguchi, A. Effect of extraction on furfural production by solid acid-catalyzed xylose dehydration in water. *J. Supercrit. Fluids* **2019**, *144*, 14–18. [[CrossRef](#)]
16. Gómez Millán, G.; Hellsten, S.; King, A.W.T.; Pokki, J.-P.; Llorca, J.; Sixta, H. A comparative study of water-immiscible organic solvents in the production of furfural from xylose and birch hydrolysate. *J. Ind. Eng. Chem.* **2019**, *72*, 354–363. [[CrossRef](#)]
17. Li, Y.; Sun, L.-L.; Cao, D.-M.; Cao, X.-F.; Sun, S.-N. One-step conversion of corn stalk to glucose and furfural in molten salt hydrate/organic solvent biphasic system. *Bioresour. Technol.* **2023**, *386*, 129520. [[CrossRef](#)] [[PubMed](#)]
18. Dai, Y.; Yang, S.; Wang, T.; Tang, R.; Wang, Y.; Zhang, L. High conversion of xylose to furfural over corncob residue-based solid acid catalyst in water-methyl isobutyl ketone. *Ind. Crops Prod.* **2022**, *180*, 114781. [[CrossRef](#)]
19. Li, X.; Liu, Q.; Luo, C.; Gu, X.; Lu, L.; Lu, X. Kinetics of furfural production from corn cob in  $\gamma$ -valerolactone using dilute sulfuric acid as catalyst. *ACS Sustain. Chem. Eng.* **2017**, *5*, 8587–8593. [[CrossRef](#)]
20. Tang, Z.; Li, Q.; Di, J.; Ma, C.; He, Y.C. An efficient chemoenzymatic cascade strategy for transforming biomass into furfurylamine with lobster shell-based chemocatalyst and mutated  $\omega$ -transaminase biocatalyst in methyl isobutyl ketone-water. *Bioresour. Technol.* **2023**, *369*, 128424. [[CrossRef](#)]
21. Wang, Y.; Delbecq, F.; Varma, R.S.; Len, C. Comprehensive study on expeditious conversion of pre-hydrolyzed alginic acid to furfural in Cu(II) biphasic systems using microwaves. *Mol. Catal.* **2018**, *445*, 73–79. [[CrossRef](#)]
22. Yong, K.J.; Wu, T.Y.; Lee, C.B.T.L.; Lee, Z.J.; Liu, Q.; Jahim, J.M.; Zhou, Q.; Zhang, L. Furfural production from biomass residues: Current technologies, challenges and future prospects. *Biomass Bioenergy* **2022**, *161*, 106458. [[CrossRef](#)]
23. Xu, Z.; Zhang, G.; Wang, K. Efficient conversion of biomass derivatives to furfural with a novel carbon-based solid acid catalyst. *Catal. Commun.* **2023**, *175*, 106608. [[CrossRef](#)]
24. Fúnez-Núñez, I.; García-Sancho, C.; Cecilia, J.A.; Moreno-Tost, R.; Serrano-Cantador, L.; Maireles-Torres, P. Recovery of pentoses-containing olive stones for their conversion into furfural in the presence of solid acid catalysts. *Process Saf. Environ. Prot.* **2020**, *143*, 1–13. [[CrossRef](#)]
25. Zhang, T.; Li, W.; An, S.; Huang, F.; Li, X.; Liu, J.; Pei, G.; Liu, Q. Efficient transformation of corn stover to furfural using *p*-hydroxybenzenesulfonic acid-formaldehyde resin solid acid. *Bioresour. Technol.* **2018**, *264*, 261–267. [[CrossRef](#)]
26. Grant, K.R.; Brennan, M.; Hoad, S.P. The structure of the Barley husk influences its resistance to mechanical stress. *Front. Plant Sci.* **2020**, *11*, 614334. [[CrossRef](#)]
27. Zhang, T.; Li, W.; Xu, Z.; Liu, Q.; Ma, Q.; Jameel, H.; Chang, H.-M.; Ma, L. Catalytic conversion of xylose and corn stalk into furfural over carbon solid acid catalyst in  $\gamma$ -valerolactone. *Bioresour. Technol.* **2016**, *209*, 108–114. [[CrossRef](#)]
28. Teng, X.; Si, Z.; Li, S.; Yang, Y.; Wang, Z.; Li, G.; Zhao, J.; Cai, D.; Qin, P. Tin-loaded sulfonated rape pollen for efficient catalytic production of furfural from corn stover. *Ind. Crops Prod.* **2020**, *151*, 112481. [[CrossRef](#)]
29. Gong, L.; Xu, Z.-Y.; Dong, J.-J.; Li, H.; Han, R.-Z.; Xu, G.-C.; Ni, Y. Composite coal fly ash solid acid catalyst in synergy with chloride for biphasic preparation of furfural from corn stover hydrolysate. *Bioresour. Technol.* **2019**, *293*, 122065. [[CrossRef](#)]
30. Yang, Q.; Fan, B.; He, Y.C. Combination of solid acid and solvent pretreatment for co-production of furfural, xylooligosaccharide and reducing sugars from *Phyllostachys edulis*. *Bioresour. Technol.* **2024**, *395*, 130398. [[CrossRef](#)] [[PubMed](#)]
31. Li, H.; Ren, J.; Zhong, L.; Sun, R.; Liang, L. Production of furfural from xylose, water-insoluble hemicelluloses and water-soluble fraction of corncob via a tin-loaded montmorillonite solid acid catalyst. *Bioresour. Technol.* **2015**, *176*, 242–248. [[CrossRef](#)] [[PubMed](#)]
32. Liao, S.; Donggen, H.; Yu, D.; Su, Y.; Yuan, G. Preparation and characterization of ZnO/TiO<sub>2</sub>, SO<sub>4</sub><sup>2-</sup>/ZnO/TiO<sub>2</sub> photocatalyst and their photocatalysis. *J. Photochem. Photobiol. A Chem.* **2004**, *168*, 7–13. [[CrossRef](#)]
33. Winoto, H.P.; Ahn, B.S.; Jae, J. Production of  $\gamma$ -valerolactone from furfural by a single-step process using Sn-Al-Beta zeolites: Optimizing the catalyst acid properties and process conditions. *J. Ind. Eng. Chem.* **2016**, *40*, 62–71. [[CrossRef](#)]
34. Luo, W.; Cao, W.; Bruijninx, P.C.A.; Lin, L.; Wang, A.; Zhang, T. Zeolite-supported metal catalysts for selective hydrodeoxygenation of biomass-derived platform molecules. *Green Chem.* **2019**, *21*, 3744–3768. [[CrossRef](#)]

35. Dietz, C.H.J.T.; Verra, M.; Verberkt, S.; Gallucci, F.; Kroon, M.C.; Neira D'Angelo, M.F.; Papaioannou, M.; van Sint Annaland, M. Sequential and in situ extraction of Furfural from reaction mixture and effect of extracting agents on furfural degradation. *Ind. Eng. Chem. Res.* **2019**, *58*, 16116–16125. [[CrossRef](#)]
36. Zhao, Y.; Xu, H.; Wang, K.; Lu, K.; Qu, Y.; Zhu, L.; Wang, S. Enhanced furfural production from biomass and its derived carbohydrates in the renewable butanone–water solvent system. *Sustain. Energy Fuels* **2019**, *3*, 3208–3218. [[CrossRef](#)]
37. Liu, Y.; Ma, C.; Huang, C.; Fu, Y.; Chang, J. Efficient conversion of xylose into furfural using sulfonic acid-functionalized metal–organic frameworks in a biphasic system. *Ind. Eng. Chem. Res.* **2018**, *57*, 16628–16634. [[CrossRef](#)]
38. Mansir, N.; Taufiq-Yap, Y.H.; Rashid, U.; Lokman, I.M. Investigation of heterogeneous solid acid catalyst performance on low grade feedstocks for biodiesel production: A review. *Energy Convers. Manag.* **2017**, *141*, 171–182. [[CrossRef](#)]
39. Ni, J.; Li, Q.; Gong, L.; Liao, X.-L.; Zhang, Z.-J.; Ma, C.; He, Y. Highly efficient chemoenzymatic cascade catalysis of biomass into furfurylamine by a heterogeneous shrimp shell-based chemocatalyst and an  $\omega$ -transaminase biocatalyst in deep eutectic solvent–water. *ACS Sustain. Chem. Eng.* **2021**, *9*, 13084–13095. [[CrossRef](#)]
40. Zha, J.; Fan, B.; He, J.; He, Y.C.; Ma, C. Valorization of Biomass to Furfural by Chestnut Shell-based Solid Acid in Methyl Isobutyl Ketone-Water-Sodium Chloride System. *Appl. Biochem. Biotechnol.* **2022**, *194*, 2021–2035. [[CrossRef](#)]
41. Hu, B.; Xie, W.-L.; Wu, Y.-T.; Liu, J.; Ma, S.-W.; Wang, T.-P.; Zheng, S.; Lu, Q. Mechanism study on the formation of furfural during zinc chloride-catalyzed pyrolysis of xylose. *Fuel* **2021**, *295*, 120656. [[CrossRef](#)]
42. Ji, L.; Tang, Z.; Yang, D.; Ma, C.; He, Y.C. Improved one-pot synthesis of furfural from corn stalk with heterogeneous catalysis using corn stalk as biobased carrier in deep eutectic solvent-water system. *Bioresour. Technol.* **2021**, *340*, 125691. [[CrossRef](#)] [[PubMed](#)]
43. Huang, T.; Zhou, Y.; Zhang, X.; Peng, D.; Nie, X.; Chen, J.; Xiong, W. Conversion of carbohydrates into furfural and 5-hydroxymethylfurfural using furfuryl alcohol resin-based solid acid as catalyst. *Cellulose* **2022**, *29*, 1419–1433. [[CrossRef](#)]
44. He, Y.; Huang, M.; Tang, W.; Ma, C. Improving enzymatic hydrolysis of sunflower straw pretreated by deep eutectic solvent with different carboxylic acids as hydrogen bond donors. *Ind. Crops Prod.* **2023**, *193*, 116157. [[CrossRef](#)]
45. Zhang, Z.G.; Yi, Y.; Lin, J.C.; Chen, D.; Ji, X.J. One-pot two-step biocatalytic upgrading of 5-hydroxymethylfurfural to 2,5-furandicarboxylic acid (FDCA) through a sequential oxidation process. *Sustain. Chem. Pharm.* **2024**, *39*, 101616. [[CrossRef](#)]
46. Zhu, X.; Liu, M.; Sun, Q.; Ma, J.; Xia, A.; Huang, Y.; Zhu, X.; Liao, Q. Elucidation of the interaction effects of cellulose, hemicellulose and lignin during degradative solvent extraction of lignocellulosic biomass. *Fuel* **2022**, *327*, 125141. [[CrossRef](#)]
47. Nayak, R.; Cleveland, D.; Tran, G.; Joseph, F. Potential of bacterial cellulose for sustainable fashion and textile applications: A review. *J. Mater. Sci.* **2024**, *59*, 6685–6710. [[CrossRef](#)]
48. Huang, C.; Lin, W.; Zheng, Y.; Zhao, X.; Ragauskas, A.; Meng, X. Evaluating the mechanism of milk protein as an efficient lignin blocker for boosting the enzymatic hydrolysis of lignocellulosic substrates. *Green Chem.* **2022**, *24*, 5263–5279. [[CrossRef](#)]
49. Tang, W.; Tang, Z.; Qian, H.; Huang, C.; He, Y.C. Implementing dilute acid pretreatment coupled with solid acid catalysis and enzymatic hydrolysis to improve bioconversion of bamboo shoot shells. *Bioresour. Technol.* **2023**, *381*, 129167. [[CrossRef](#)]

**Disclaimer/Publisher's Note:** The statements, opinions and data contained in all publications are solely those of the individual author(s) and contributor(s) and not of MDPI and/or the editor(s). MDPI and/or the editor(s) disclaim responsibility for any injury to people or property resulting from any ideas, methods, instructions or products referred to in the content.